Toward Cost-Efficient and Reliable Unit Commitment Under Uncertainty

Hrvoje Pandžić, *Member, IEEE*, Yury Dvorkin, *Student Member, IEEE*, Ting Qiu, *Student Member, IEEE*, Yishen Wang, *Student Member, IEEE*, and Daniel S. Kirschen, *Fellow, IEEE*

***Abstract*—Large-scale integration of wind farms causes volatile bus net injections. Although these fluctuations are anticipated, their timing, magnitude and duration cannot be predicted accurately. In order to maintain the operational reliability of the system, this uncertainty must be adequately addressed at the day-ahead generation scheduling stage. The ad-hoc reserve rules incorporated in deterministic unit commitment formulations do not adequately account for this uncertainty. Scenario-based stochastic unit commitment formulations model this uncertainty more precisely, but require computationally demanding simulations. Interval and robust optimization techniques require less computing resources, but produce overly conservative and thus expensive generation schedules. This paper proposes a transmission-constrained unit commitment formulation that improves the performance of the interval unit commitment. The uncertainty is modeled using upper and lower bounds, as in the interval formulation, but inter-hour ramp requirements are based on net load scenarios. This improved interval formulation has been tested using the IEEE RTS-96 and compared with existing stochastic, interval and robust unit commitment techniques in terms of solution robustness and cost. These results show that the proposed method outperforms the existing interval technique both in terms of cost and computing time.**

***Index Terms*—Interval optimization, stochastic optimization, uncertainty, unit commitment.**

I. Introduction

A. Background

As electricity generation from renewable resources, such as solar and wind generation increases, power system operators (SO) must increase reserve margins to account for the larger uncertainty on the net load [1], [2]. Although the accuracy of forecasting tools has improved [3], ex-post analyses of wind forecast errors reveal that they increase non-linearly for lead times of over 6 h [4]. These forecasting errors require significantly larger reserve margins [5], which increase the overall operating cost [6]. Furthermore, existing power systems have not been designed to effectively withstand these levels of uncertainty and may therefore require sizable investments to make their generation fleet more flexible [7]. In order to maintain the operational reliability of the system and simultaneously avoid high generation costs, a computationally effective approach is needed to select the most cost-effective combination of controllable generators that can effectively respond to the fluctuations of the intermittent power producers.

The day-ahead reliability unit commitment (UC) is an optimization problem that produces physical generator commitment decisions that minimize the cost of serving forecasted net load subject to operational constraints on generation resources and transmission lines [8]. In this paper, the term net load is defined as the difference between the load and the output of renewable generation.

In the deterministic UC (DUC) formulation, the net load is modeled by a single forecast and the associated uncertainty is handled using ad-hoc reserve rules [1], [9]–[12]. Such an approach to the provision of reserve does not involve an endogenous cost/benefit or probabilistic analysis of the reserve requirements as advocated in [13]–[15]. This leads to sub-optimal commitment decisions when actual conditions deviate significantly from the assumptions made when the reserve requirements policy is set [16], [17]. The authors of [18] and [19] show that accounting for multiple forecasts (or scenarios) in the UC reduces the operating cost. Efficient Stochastic UC (SUC) formulations [21]–[25] have been developed on the basis of sophisticated wind scenario generation techniques [20]. These formulations minimize the expected operating cost over all scenarios, weighing the cost of each scenario in proportion to its likelihood. Typically, the SUC is formulated as a two-stage optimization problem [26]. First, here-and-now decisions are made on the binary status of generators. These decisions are common to all scenarios. Wait-and-see decisions on the dispatch of each generator committed at the first stage are then made separately for each scenario.

However, the solution of the SUC is computationally demanding when the problem involves a large power system or a moderate number of scenarios. This issue can be somewhat mitigated if the set of scenarios is reduced using a scenario reduction technique [27]–[30]. However, an insufficient number of scenarios reduces the accuracy of the solution and increases its cost [27], [31], [32]. The relationship between the number of scenarios and the SUC solution is studied in [27]. Reference [32]

Manuscript received June 24, 2014; revised November 10, 2014, February 22, 2015, and April 21, 2015; accepted May 15, 2015. This work was supported in part by the ARPA-E Green Electricity Network Integration (GENI) program under project DE-FOA-0000473 and in part by the State of Washington STARS program. Paper no. TPWRS-00855-2014.

H. Pandžić is with the Faculty of Electrical Engineering and Computing, University of Zagreb, Zagreb, Croatia (e-mail: hrvoje.pandzic@ieee.org).

Y. Dvorkin, T. Qiu, Y. Wang, and D. S. Kirschen are with the Department of Electrical Engineering, University of Washington, Seattle, WA 98105 USA (e-mail: dvorkin@uw.edu; tqiu@uw.edu; ywang11@uw.edu; kirschen@uw.edu).

Color versions of one or more of the figures in this paper are available online at http://ieeexplore.ieee.org.

Digital Object Identifier 10.1109/TPWRS.2015.2434848

studies the impact of different scenario reduction techniques on the SUC model and compares its performance to the IUC model. The two-stage structure of the SUC can be exploited to improve its computational performance using Benders' decomposition [23], [24] or progressive hedging [33].

In the robust UC (RUC) formulations, upper and lower bounds on the net load at each optimization interval define the range of uncertainty. This definition thus ignores the probability of a particular realization of uncertainty within the given range. The RUC enforces the feasibility of its schedule over a given uncertainty set and minimizes the dispatch cost under the worst-case realization [34]. The worst-case realization is determined endogenously and thus simultaneously accounts for both unfavorable magnitudes and high ramp rates within the range of net loads. Like the SUC, the RUC also has a two-stage structure and therefore can be implemented using the Benders decomposition [34]–[37] or the column-and-constraint generation method [38], [39]. The latter method improves the computational performance of the RUC model and reduces the number of iterations required to obtain the optimal solution, while ensuring the same cost performance as the Benders decomposition [38]. Unlike the SUC, the RUC is tractable for a large interconnection [34] and its computational burden mainly results from solving an inner max-min problem that seeks the worst-case realization of uncertainty. The conservatism of the RUC can be adjusted using the budget of uncertainty. In [34], the budget of uncertainty is defined as the number of buses that are allowed to deviate from a given central wind forecast in the worst-case scenario. The value for the budget of uncertainty must be specified before solving the RUC model. Until the RUC is solved, it is unknown which buses will be chosen by the RUC model to deviate from the central wind forecast.

The Interval UC (IUC) [47], [48] produces a schedule that minimizes the cost of serving the most probable (central) net load forecast while guaranteeing that any realization of uncertainty within a given range around this central forecast will not require changes in the commitment. As in the RUC, this range is delimited by its upper and lower bounds. As compared to the RUC, which endogenously determines the worst-case realization, the IUC formulation enforces transitions from the upper to the lower bound between any two consecutive optimization intervals by means of deterministic constraints [48]. Unlike the RUC, which optimizes the cost of its decisions for the worst-case scenario, the IUC minimizes the operating cost of the central forecast. If the IUC and RUC are solved for the same range of uncertainty, their commitment and dispatch decisions may vary unless the worst-case scenario in the RUC matches the central forecast in the IUC. Since the commitment and dispatch decisions of the IUC and RUC are different, these two formulations will also exhibit different sensitivities to real-time adjustments. In line with the SUC and RUC, the IUC can also be implemented using the Benders' decomposition [31], [48]. The IUC produces more conservative schedules than the SUC, but requires less computing resources [31]. As compared to the RUC, the IUC model avoids solving an inner max-min optimization and, thus, its second stage can be formulated as an LP problem, if the first stage binary decisions are fixed. The common thread of the SUC and IUC models is that the generation-load balance is enforced for a limited number of scenarios. On the other hand, the RUC model ensures that this balance is maintained for any realization within a pre-defined uncertainty set. Therefore, the RUC model offers a more methodologically rigorous approach to ensuring adequate reserve margins.

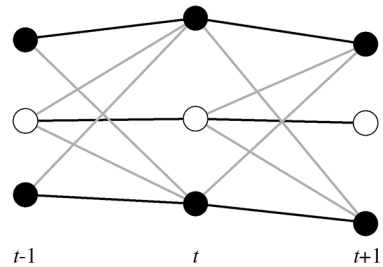

Fig. 1. IUC scenarios (black) with transition constraints (grey).

A unified stochastic and robust UC formulation has been proposed in [40] to reduce the conservatism of the RUC. However, this approach employs heuristics to balance the SUC and RUC solutions, which may result in a suboptimal solution. This issue is overcome in the hybrid stochastic/interval UC model [41]. This approach enforces the SUC for operating hours at the beginning of the optimization horizon and then switches to the interval formulation for the remaining hours. The switching time is optimized to achieve the optimal trade-off between the cost of unhedged uncertainty from the SUC and the security premium of the IUC.

Zheng *et al.* [42] present a detailed literature review on stochastic and robust formulations of UC problems, including a number of solution techniques that reduce the computing times. However, these techniques may also introduce some ambiguity in the settlement process and pricing, and cause numerical instability [43] and convergence issues [44]. These challenges are currently being investigated by SOs [42], [45], [46].

B. Proposed Method and Contributions

The IUC formulation is computationally more efficient than the SUC because the generation uncertainty of each wind farm is represented by only three non-probabilistic scenarios (black lines in Fig. 1): the central forecast (white circles) and the lower bound and the upper bounds (black circles). On the other hand, IUC solutions are more conservative because of the constraints that it imposes on the feasibility of transitions from lower to upper bound, and vice versa, between any two consecutive time periods, as illustrated by the grey lines in Fig. 1. Such extreme transitions have a very low probability and can be replaced by less severe ramp constraints. Since scenarios are designed to accurately capture the characteristics of the expected wind output, we argue that the required rampable capacity should be no more than the maximum up and down ramps observed over all stochastic scenarios. However, if ramping constraints would be completely relaxed, the day-ahead solution would be very vulnerable to wind volatility and the overall cost of running a system would be high.

Fig. 2 illustrates the difference between modeling of wind scenarios and bounds for each wind farm in SUC, IUC and this Improved Interval UC (IIUC). Fig. 2(a) shows the scenarios

used by the SUC. Bounds for both IUC and IIUC are created based on the minimum and maximum values of these scenarios at each hour. For instance, scenario s1 sets the lower bound in hours 1–4 and 6, while the lower bound in hour 5 is set by scenario s2. Fig. 2(b) shows the IUC bounds, as well as the up and down ramp requirements. The central forecast and its ramp constraints are omitted for clarity. Fig. 2(c) shows artificial IIUC scenarios, which correspond to ramp requirements between consecutive hours. Each of these ramps ends at one of the bounds, while the location of its *tail* at the hour before is determined based on the highest slope over all stochastic scenarios. This way each dotted segment in Fig. 2(c) defines up ramp requirement and upper bound, while each dashed segment defines down ramp requirement and lower bound. For example, the up ramp requirement between hours 1 and 2 is 10 MW/h because the highest ramp of the three stochastic scenarios in Fig. 2(a) is 10 MW/h (s2 and s3). Since the upper bound at hour 2 is 50 MW, the first dotted segment starts at 40 MW in hour 1 and ends at 50 MW in hour 2. Similarly, up ramp requirement between hours 2 and 3 is 20 MW/h (set by scenario s2) and it ends at the upper bound (60 MW). The remaining up ramp requirements are 30 MW/h between hours 3 and 4 (set by s3), 10 MW/h between hours 4 and 5 (set by s1), and again 10 MW/h between hours 5 and 6 (set by s2). The corresponding upper bounds are 80 MW, 80 MW, and 70 MW, respectively. On the other hand, the first four down ramp requirements are equal to zero because this is the largest down ramp observed over all three stochastic scenarios during these 5 hours. The down ramp requirement between hours 5 and 6 is -10 MW/h, as determined by scenarios s1 and s3. All dashed lines end on lower bounds determined by the stochastic scenarios from Fig. 2(a). To obtain ramp requirements and bounds for each wind farm in a given power system, the methodology explained in Fig. 2 is applied to each wind farm individually.

A single scenario[1] cannot be used for all up ramp limits as this would result in two operating points at each time period (one at the upper bound, which is the end point of the ramp requirement between the previous and the current hour, and one below it, which is the tail point of the ramp limit between the current and the following hour). For this reason, the IIUC is formulated using five scenarios: u_1—the central forecast, whose cost is minimized in the objective function; u_2—up ramp limits between odd and even hours; u_3—up ramp limits between even and odd hours; u_4—down ramp limits between odd and even hours; u_5—down ramp limits between even and odd hours.

Because the ramp constraints are less demanding, the IIUC produces less conservative generator schedules than the IUC.

This paper makes the following contributions:

1) It proposes a new IIUC formulation that aims to improve the day-ahead reliability unit commitment procedures and combines aspects of SUC and IUC. This model takes advantage of the cost-efficient SUC model and the computational simplicity of the IUC model.
2) It demonstrates the effectiveness of the IIUC based on extensive tests with various wind penetration levels, wind profiles and controllable generator characteristics.
3) It also provides a systematic and rigorous comparative assessment of the cost and reliability performance of the IIUC, IUC, RUC, and SUC formulations. As to the best of the authors' knowledge, such a comparison has not been performed for these UC approaches on the same set of data.

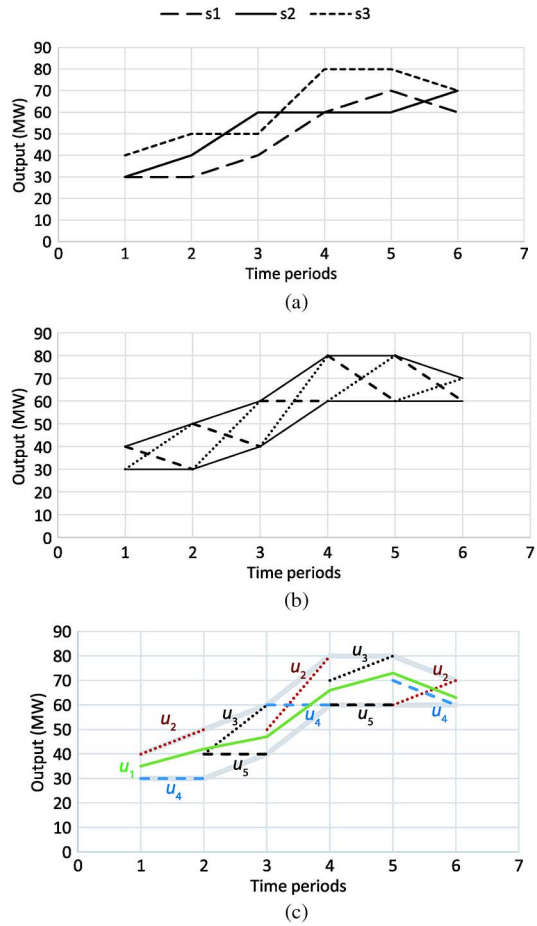

Fig. 2. Illustrative example of uncertainty modeling: (a) scenarios used in SUC; (b) bounds (lines), up ramp requirements (dotted lines) and down ramp requirements (dashed lines) used in IUC; (c) central forecast (green line), bounds (thick grey lines), up ramp requirements (dotted lines) and down ramp requirements (dashed lines) used in IIUC.

II. Formulation

To ensure a fair comparison between the IIUC, IUC, RUC, and SUC in terms of both cost and computing time, all constraints have been implemented in the same way except where these formulations differ. The formulation of the IIUC is presented first. The other techniques are then defined in terms of how they differ from the IIUC.

A. Notation

1) Sets:

Ω^{B}	Set of piecewise linear segments of each generating unit's cost curve, indexed by b.
Ω^{I}	Set of generating units, indexed by i.
Ω^{J}	Set of generating units' start-up costs, indexed by j.
Ω^{L}	Set of transmission lines, indexed by l.

[1]The term *scenarios* should be used with reservations, as *scenarios* in IIUC are used for modeling purposes only, and they do not consider probability.

Ω^{R} Set of uncertainty for the RUC, indexed by r.
Ω^{S} Set of buses, indexed by s.
Ω^{T} Set of hours, indexed by t.
Ω^{U} Set of scenarios, indexed by u.
Ω^{X} Set of feasible dispatch solutions for fixed commitment decisions $\mathbf{x}$, such that $\mathbf{x} = \{x_{t,i}\}$, $\forall t \in \Omega^T, i \in \Omega^I$.
Ω^{W} Set of wind farms, indexed by w.

2) Binary Variables:

$q_{t,i,j}$ Generator start-up cost identification matrix (1 if generator i is started up during hour t after being off for $\underline{T}_{i,j}$ to $\overline{T}_{i,j}$ hours, 0 otherwise).
$x_{t,i}$ Generator on/off status (1 if generator i is on during hour t, 0 otherwise).
$y_{t,i}$ Generator start-up status (1 if generator i is started up during hour t, 0 otherwise).
$z_{t,i}$ Generator shut down status (1 if generator i is shut down during hour t, 0 otherwise).

3) Continuous non-Negative Variables:

$c_{t,w,u}$ Power curtailment of wind farm w under scenario u during hour t (MW).
$g_{t,i,u}$ Power output of generator i under scenario u during hour t (MW).
$g^{\mathrm{seg}}_{t,i,b,u}$ Power output on segment b of generator i under scenario u during hour t (MW).
$su_{t,i}$ Start-up cost of generator i during hour t (\$).

4) Continuous Variables:

$\theta_{t,s,u}$ Voltage angle at bus s under scenario u during hour t (rad).

5) Parameters:

A_i No-load cost of generator i (\$).
B_{sm} Admittance of line connecting nodes s and m (S).
$D_{t,s}$ Load at bus s during hour t (MW).
DT_i Generator i minimum down time (h).
$\overline{G}_i$ Maximum power output of generator i (MW).
$\underline{G}_i$ Minimum power output of generator i (MW).
$K_{i,b}$ Slope of the bth segment of the cost curve of generator i (\$/MW).
$\overline{L}_i$ Minimum up time of generator i (h).
$\underline{L}_i$ Minimum down time of generator i (h).
L_{sm} Capacity of the line connecting nodes s and m (MW).
RD_i Ramp down limit of generator i (MW/h).
RU_i Ramp up limit of generator i (MW/h).
$SUC_{i,j}$ Cost of segment j of the stepwise start-up cost curve of generator i (\$).
$\overline{T}_{i,j}$ Upper limit of segment j of the stepwise start-up cost curve of generator i (h).
$\underline{T}_{i,j}$ Lower limit of segment j of the stepwise start-up cost of generator i curve (h).
UT_i Generator i minimum up time (h).
$W_{t,w,u}$ Available wind power at wind farm w under scenario u during hour t (MW).
π_u Probability of scenario u (used only in the SUC).

B. Formulation of the IIUC

The objective function of the IIUC aims to minimize the operating cost of the central forecast scenario u_1 and includes the no-load cost, the start-up cost and the running cost of all the generators:

$$\min_{\substack{q_{t,i,j},x_{t,i},y_{t,i},z_{t,i},\\ c_{t,w,u},g_{t,i,u},g^{\mathrm{seg}}_{t,i,b,u},su_{t,i},\theta_{t,s,u}}} \sum_{t\in\Omega^{\mathrm{T}}}\sum_{i\in\Omega^{\mathrm{I}}} \Big[su_{t,i} + A_i \cdot x_{t,i} + \sum_{b\in\Omega^{\mathrm{B}}} K_{i,b}\cdot g_{t,i,b,u_1}\Big]. \quad (1)$$

The choice of this objective function is motivated by the IUC model [23]. Since objective function (1) minimizes the operating cost of the central forecast, the actual materialization of uncertainty, which is expected to differ from the central forecast, will require real-time re-dispatch, which may cause additional expenses as compared to the central forecast [31]. However, the case study in [31] performed on the 118-bus IEEE RTS shows that these expenses are of the same order as those resulting from the application of a SUC optimization.

This optimization is subject to the following constraints:

1) Binary Variables Logic:

$$y_{t,i} - z_{t,i} = x_{t,i} - x_{t-1,i}, \quad \forall t \in \Omega^{\mathrm{T}}, i \in \Omega^{\mathrm{I}} \quad (2)$$
$$y_{t,i} + z_{t,i} \le 1, \quad \forall t \in \Omega^{\mathrm{T}}, i \in \Omega^{\mathrm{I}}. \quad (3)$$

Constraint (2) determines if generator i is started up or shut down at time t based on the change of its 0/1 status between hours $t-1$ and t. Constraint (3) ensures that generator i cannot be started up and shut down during the same time period.

2) Minimum Up and Down Times:

$$x_{t,i} = x_{t_0,i}, \quad \forall t \in [0, \overline{L}_i + \underline{L}_i], i \in \Omega^{\mathrm{I}} \quad (4)$$
$$\sum_{r=t-UT_i+1}^{t} y_{r,i} \le x_{t,i}, \quad \forall t \in [\overline{L}_i, T], i \in \Omega^{\mathrm{I}} \quad (5)$$
$$\sum_{r=t-DT_i+1}^{t} z_{r,i} \le 1 - x_{t,i}, \quad \forall t \in [\underline{L}_i, T], i \in \Omega^{\mathrm{I}}. \quad (6)$$

Constraint (4) sets the on/off status for the first $\overline{L}_i + \underline{L}_i$ hours based on the initial status of the generators. For example, if a generator must stay on for three hours, $\overline{L}_i$ will be 3, and $\underline{L}_i$ will be 0. If no minimum up or down time constraints are active at the beginning of the scheduling horizon, both $\overline{L}_i$ and $\underline{L}_i$ will be 0. Constraints (5) and (6) enforce minimum up and down time for the remaining time intervals as explained in [49].

3) Stepwise Generator Start-Up Cost:

$$q_{t,i,j} \le \sum_{r=\underline{T}_{i,j}}^{\overline{T}_{i,j}} z_{t-r,i}, \quad \forall t \in \Omega^{\mathrm{T}}, i \in \Omega^{\mathrm{I}}, j \in \Omega^{\mathrm{J}} \quad (7)$$
$$\sum_{j\in\Omega^{\mathrm{J}}} q_{t,i,j} = y_{t,i}, \quad \forall t \in \Omega^{\mathrm{T}}, i \in \Omega^{\mathrm{I}} \quad (8)$$

$$su_{t,i} = \sum_{j \in \Omega^{\mathrm{J}}} SUC_{i,j} \cdot q_{t,i,j}, \quad \forall t \in \Omega^{\mathrm{T}}, i \in \Omega^{\mathrm{I}}. \quad (9)$$

The start-up cost of each generator depends on the number of hours it has been off. Constraint (7) identifies the appropriate segment of the start-up cost curve to be used based on the number of hours the generator has been off. Constraint (8) ensures that exactly one element j of $q_{t,i,j}$ is assigned the value 1 if $y_{t,i} = 1$. The actual start-up cost is set by constraint (9).

4) Generator Constraints:

$$g_{t,i,u} = \sum_{b \in \Omega^{\mathrm{B}}} g^{\mathrm{seg}}_{t,i,b,u}, \quad \forall t \in \Omega^{\mathrm{T}}, i \in \Omega^{\mathrm{I}}, u \in \Omega^{\mathrm{U}} \quad (10)$$

$$\underline{G}_i \cdot x_{t,i} \leq g_{t,i,u} \leq \overline{G}_i \cdot x_{t,i}, \quad \forall t \in \Omega^{\mathrm{T}}, i \in \Omega^{\mathrm{I}}, u \in \Omega^{\mathrm{U}} \quad (11)$$

$$-RD_i \leq g_{t,i,u_1} - g_{t-1,i,u_1} \leq RU_i, \quad \forall t \in \Omega^{\mathrm{T}}, i \in \Omega^{\mathrm{I}} \quad (12)$$

$$g_{t,i,u_2} - g_{t-1,i,u_2} \leq RU_i, \quad \forall t \in \Omega^{\mathrm{T}} \,|\, t \equiv 0(\mathrm{mod}2), i \in \Omega^{\mathrm{I}} \quad (13)$$

$$g_{t,i,u_3} - g_{t-1,i,u_3} \leq RU_i, \quad \forall t \in \Omega^{\mathrm{T}} \,|\, t \equiv 1(\mathrm{mod}2), i \in \Omega^{\mathrm{I}} \quad (14)$$

$$-RD_i \leq g_{t,i,u_4} - g_{t-1,i,u_4}, \quad \forall t \in \Omega^{\mathrm{T}} \,|\, t \equiv 0(\mathrm{mod}2), i \in \Omega^{\mathrm{I}} \quad (15)$$

$$-RD_i \leq g_{t,i,u_5} - g_{t-1,i,u_5}, \quad \forall t \in \Omega^{\mathrm{T}} \,|\, t \equiv 1(\mathrm{mod}2), i \in \Omega^{\mathrm{I}}\,. \quad (16)$$

Equation (10) defines the power output of each generator as the sum of the output on each segment of its cost curve. Constraint (11) enforces the minimum and maximum generator output limits. Constraint (12) enforces the up and down ramp limits for the central forecast scenario u_1. Constraint (13) enforces the up ramp limits for scenario u_2, i.e., only between odd and even hours, while constraint (14) enforces these up ramp limits for scenario u_3, i.e., only between even and odd hours. This is implemented using the modulo function, which returns 0 for even time periods (remainder when dividing an even number by 2 is 0), and 1 for odd time periods (remainder when dividing an odd number by 2 is 1). Similarly, constraints (15) and (16) enforce the down ramp limits for scenarios u_4 (between odd and even hours) and u_5 (between even and odd hours).

5) Transmission Constraints:

$$\sum_{i \in \Omega^{\mathrm{S}}} g_{t,i,u} + \sum_{w \in \Omega^{\mathrm{S}}} (W_{t,w,u} - c_{t,w,u}) - \sum_{\{s,m\} \in \Omega^{\mathrm{L}}} B_{sm}(\theta_{t,s,u} - \theta_{t,m,u}) = D_{t,s}, \quad \forall t \in \Omega^{\mathrm{T}}, s \in \Omega^{\mathrm{S}}, u \in \Omega^{\mathrm{U}} \quad (17)$$

$$0 \leq c_{t,w,u} \leq W_{t,w,u}, \forall t \in \Omega^{\mathrm{T}}, w \in \Omega^{\mathrm{W}}, u \in \Omega^{\mathrm{U}} \quad (18)$$

$$-L_{sm} \leq B_{sm}(\theta_{t,m,u} - \theta_{t,s,u}) \leq L_{sm}, \quad \forall t \in \Omega^{\mathrm{T}}, \{s,m\} \in \Omega^{\mathrm{L}}, u \in \Omega^{\mathrm{U}} \quad (19)$$

$$-\pi \leq \theta_{t,s,u} \leq \pi, \forall t \in \Omega^{\mathrm{T}}, s \in \Omega^{\mathrm{S}} \backslash s_{\mathrm{ref}}, u \in \Omega^{\mathrm{U}} \quad (20)$$

$$\theta_{t,s_{\mathrm{ref}}} = 0, \forall t \in \Omega^{\mathrm{T}}. \quad (21)$$

Equation (17) enforces the nodal power balance. Equation (18) limits the amount of wind spillage at each wind farm. If the line flow limits imposed by (19) cannot be met for a given value of the available wind power at wind farm w, the available wind power will be curtailed by $c_{t,w,u}$. Equation (20) limits the voltage angles while (21) sets the voltage angle to zero at the reference bus. To ensure the feasibility of the IIUC model, equation (17) can be relaxed over all scenarios, but the central forecast scenario. The slack variables should then be penalized in the objective function based on [41], which complies with practices of system operators [34],[50]. Furthermore, if these slack variables turn out to be non-zero, these cases should be carefully examined to avoid load shedding in real-time.

C. Formulation of the IUC

The IUC is modeled using three scenarios: u_1 is the central forecast (as in the IIUC), u_2 is the upper bound, and u_3 is the lower bound. Additional constraints are used to enforce the feasibility of the transitions between bounds (grey lines in Fig. 1).

The objective function and all the constraints are modeled as in the IIUC formulation, except for the ramp constraints (12)–(16) which are replaced by the following constraints, as in [48]:

$$-RD_i \leq g_{t,i,u_1} - g_{t-1,i,u_1} \leq RU_i, \quad \forall t \in \Omega^{\mathrm{T}}, i \in \Omega^{\mathrm{I}} \quad (22)$$

$$g_{t-1,i,u_1} - g_{t,i,u_3} \leq RD_i, \quad \forall t \in \Omega^{\mathrm{T}}, i \in \Omega^{\mathrm{I}} \quad (23)$$

$$-g_{t-1,i,u_1} + g_{t,i,u_2} \leq RU_i, \quad \forall t \in \Omega^{\mathrm{T}}, i \in \Omega^{\mathrm{I}} \quad (24)$$

$$g_{t-1,i,u_2} - g_{t,i,u_3} \leq RD_i, \quad \forall t \in \Omega^{\mathrm{T}}, i \in \Omega^{\mathrm{I}} \quad (25)$$

$$-g_{t-1,i,u_3} + g_{t,i,u_2} \leq RU_i, \quad \forall t \in \Omega^{\mathrm{T}}, i \in \Omega^{\mathrm{I}}. \quad (26)$$

Constraint (22) enforces both the up and down ramp limits on the central forecast scenario u_1. Constraints (23) and (24) enforce the transitions from the central forecast scenario to the lower (u_3) and upper (u_2) bound scenarios, respectively. Transition requirements between the upper and lower bounds are enforced by constraints (25) and (26). Therefore, inequalities (22)–(26) model all possible transitions in a given uncertainty range, as illustrated in Fig. 1. However, constraints (23) and (24) can be removed from the original IUC model in [48], since they hold automatically because of constraints (25) and (26).

D. Formulation of the SUC

The objective function of the SUC weighs the cost of each scenario in proportion to its likelihood:

$$\min_{\substack{q_{t,i},x_{t,i},y_{t,i},z_{t,i},\\ su_{t,i},g_{t,i,u},g^{\mathrm{seg}}_{t,i,b,u},c_{t,w,u},\theta_{t,s,u}}} \left[\sum_{t \in \Omega^{\mathrm{T}}} \sum_{i \in \Omega^{\mathrm{I}}} A_i \cdot x_{t,i} + su_{t,i} + \sum_{u \in \Omega^{\mathrm{U}}} \pi_u \sum_{b \in \Omega^{\mathrm{B}}} K_{i,b} \cdot\ g_{t,i,b,u} \right]. \quad (27)$$

The constraints, with the exception of the ramp constraints, are the same as in the IIUC formulation. However, the set of SUC scenarios contains actual scenarios, instead of the central scenario and artificial scenarios, such as IIUC and IUC. Ramp constraints (12)–(16) are replaced by constraint (28), which enforces ramp limits for each scenario individually:

$$-RD_i \leq g_{t,i,u} - g_{t-1,i,u} \leq RU_i, \quad \forall t \in \Omega^{\mathrm{T}}, i \in \Omega^{\mathrm{I}}. \quad (28)$$

E. Formulation of the RUC

The objective function of the RUC is formulated as in [34]:

$$\min_{\substack{q_{t,i},x_{t,i},y_{t,i},z_{t,i},\\ su_{t,i},g_{t,i,b},g^{\text{seg}}_{t,i,b},c_{t,w},\theta_{t,s}}} \left[\sum_{t\in\Omega^{\text{T}}} \sum_{i\in\Omega^{\text{I}}} su_{t,i} + A_i \cdot x_{t,i} + \max_{r\in\Omega^{\text{R}}} \sum_{b\in\Omega^{\text{B}}} K_{i,b} \cdot g_{t,i,b}(r) \right]. \quad (29)$$

The first two terms of this objective function represent the start-up cost and the no-load cost of committed generators. The third term represents the worst-case dispatch cost. Next, reference [34] recasts the worst-case dispatch term in (29) to make it solvable by existing numerical algorithms:

$$\min_{q_{t,i},x_{t,i},y_{t,i},z_{t,i},su_{t,i}} \left[\sum_{t\in\Omega^{\text{T}}} \sum_{i\in\Omega^{\text{I}}} su_{t,i} + A_i \cdot x_{t,i} + \max_{r\in\Omega^{\text{R}}} \min_{g_{t,i,b},g^{\text{seg}}_{t,i,b},c_{t,w,u},\theta_{t,s}\in\Omega^{\text{X}}} \sum_{b\in\Omega^{\text{B}}} K_{i,b} \cdot g_{t,i,b} \right]. \quad (30)$$

The worst-case dispatch term in (30) can be interpreted as the minimum economic dispatch cost for a fixed commitment $\mathbf{x}$ of all generators maximized over the uncertainty set Ω^{R} [34]. Constraints on the start-up cost and binary logic decisions are modeled as in (2)–(9), and constraints on the generation dispatch and transmission limits are modeled as in (10)–(21) with one scenario, representing the worst case for a given Ω^{R}. The RUC model is solved using the decomposition approach proposed in [34] and uses the same upper and lower bounds as the IUC and IIUC formulations. To control the conservatism of the RUC model, the budget of uncertainty is defined as $\Gamma \in \{0, 1, 2, \ldots, \text{card}(\Omega^{\text{W}})\}$, where Γ is the number of wind farms that are allowed to deviate from their central forecast. $\Gamma = 0$ means that no wind farm deviates from its central forecast, i.e., in this case the RUC model reduces to the deterministic UC model that considers only the central forecast. On the other hand, $\Gamma = \text{card}(\Omega^{\text{W}})$ stands for the most conservative case, where all wind farms can attain any value within the given uncertainty range. In this work the uncertainty set is modeled as described in [34]; however, a concept called "dynamic uncertainty sets" can be used to model temporal and spatial correlations of wind power generation more accurately [51].

III. Test Results

A. Description of the Test Cases

All four UC formulations were tested using the IEEE RTS-96 [52] modified to accommodate 19 wind farms. To create additional congestion, the original line flow limits were reduced by 20%. Fig. 3 shows the first day of the annual load data and two wind profiles that aggregate wind generation at all wind farms. These wind profiles are calculated as the sum of the central forecasts of all wind farms; therefore, the shape of the central forecast at a particular wind farm may deviate from this aggregated profile. The first aggregated wind profile in Fig. 3 roughly coincides with the load profile and is thus favorable, while the second peaks during a period of low load and is thus unfavorable. Wind energy penetration levels ranging from 10 to 50% in 10% increments were considered. All the data used for these test cases, as well as the GAMS codes for the IIUC, IUC, RUC, and SUC formulations are available at [53]. Since there is no systematic approach to choose the best Γ for the RUC model, subsection III-C assumes that $\Gamma = \text{card}(\Omega^{\text{W}})$, i.e., the optimal solution is hedged against the whole range of uncertainty at every wind farm in set Ω^{W}. Subsection III-D compares the proposed IIUC model and the RUC model with different values of Γ.

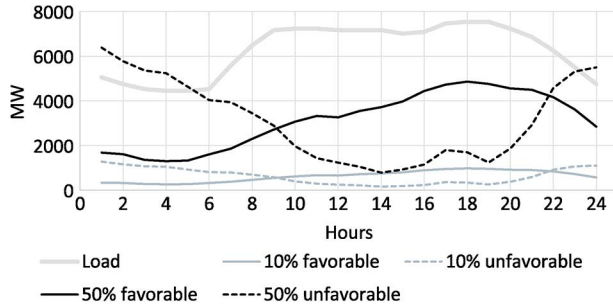

Fig. 3. Aggregated load and wind profiles used for the test cases.

Two sets of generator data were used to study the influence of generation characteristics. The first set of generator data is described in [54] and is denoted G1 in the remainder of this paper. The second set, denoted G2, uses minimum output limits, minimum up/down times and ramp limits from [55]. Generator dataset G1 has higher ramping capabilities than G2, but also higher minimum generator outputs and longer minimum up/down times. Generator types, capacities and locations are the same for both generator datasets. The total nameplate capacity of all conventional generators in G1 and G2 datasets is 10 215 MW, while the peak load during the day is 7540 MW.

B. Wind Data

An approach combining multiple statistical methods [56] was used to obtain an ensemble of 1000 wind generation scenarios for each wind farm. Note the ensemble of scenarios obtained from different scenario generation algorithms leads to lower forecasting errors than using a single scenario generation algorithm [57]. Each of the following statistical algorithms was used to produce 250 scenarios: regularized linear regression [58], support vector regression [59], multi-layer perceptron [60], and random forest [61]. These algorithms use historical wind power and speed data to generate wind power scenarios in a non-parametric manner, which avoids making any assumption that wind forecast errors follow a known distribution (e.g., Normal, Cauchy, skew-Laplace, etc.). These algorithms also ensure better fitting of the historical data to nonlinear wind turbine power curves [62]. Information regarding the geographical location of the wind farms is used to characterize the spatial correlations between them. The central forecast, W_{t,w,u_1}, for each wind farm is then calculated as the average of the 1000 scenarios in the ensemble. Since the central forecast for each wind farm is generated using same statistical algorithms and the same estimation parameters, it naturally reflects the temporal correlations. Thus, no Gaussian copula is needed.

This approach to model wind generation scenarios and the central forecast is based on processing empirical (historical) observations and, thus, avoids making any assumption on the distribution of wind generation. Since the tractability of the SUC deteriorates as the number of scenarios increases [32], the original ensemble of 1000 scenarios for each wind farm was reduced to 10 scenarios using the fast forward selection algorithm [3]. As shown in [31],[32],and [41], the choice of 10 scenarios for each wind farm represents a suitable trade-off between the computational complexity of the SUC and its cost performance. The choice of the fast forward selection algorithm is justified by its better cost and computational performance as compared to other scenario reduction techniques [32]. Instead of modeling a set of scenarios for each wind farm, the IIUC, IUC, and RUC formulations enforce the range of uncertainty for each wind farm, which hedges the optimal solution against deviations within a predetermined region covered by these scenarios. The lower and upper bounds of this range for the IIUC, IUC, and RUC models were set for each time step at the 5th and 95th percentile of the empirical probability distribution of the original ensemble of 1000 scenarios. Reference [32] proves via Monte Carlo simulations that using the original ensemble of 1000 scenarios for deriving these bounds instead of the reduced 10 scenario set enforced in the SUC results in a more cost-effective schedule.

The NREL Western Wind dataset [63] provided the wind data. Wind farm locations were mapped to the IEEE-RTS 96 respecting the lengths of the lines.

C. Cost and Reliability Performance

The day-ahead schedules produced by each formulation were tested using Monte Carlo simulations against realizations of wind uncertainty. These realizations are different from the ensemble of scenarios used for day-ahead decision-making to account for the imperfection of wind prediction tools and were generated for each wind farm as the sum of its central forecast, calculated as explained in subsection III-B, and the historical error of the central forecast for this location. Therefore, the simulated realization of wind uncertainty, $W_{t,w}^{MC}$, can be formally defined as $W_{t,w}^{MC} = W_{t,w,u_1} + \epsilon_{t,w}$, where W_{t,w,u_1} is the central forecast and $\epsilon_{t,w}$ its historical error. In line with [6] and [64], $\epsilon_{t,w}$ was sampled from a multivariate normal distribution, $\epsilon_{t,w} \sim N(\mu^w, \Sigma^w)$, where μ^w is the vector of historical forecasting error means for each operating hour and Σ^w is the covariance matrix, obtained from historical data as explained in [6]. Note that other distributions can be used to sample the error of the wind power central forecast (e.g., the Cauchy distribution [65] and the Skew-Laplace distribution [66]). In this work, the selection of the normal distribution is based on the Kolmogorov-Smirnov goodness-of-fit test, which indicates that the normal distribution may fit this forecast error better than other distributions, if ramp rates are taken into account [5]. The number of realizations required for each day-ahead schedule is calculated using the variance reduction method to achieve an error lower than 1% with a confidence of 95% [67]. This method assumes that the minimum number of realizations will vary for each day-ahead schedule depending on its cost distribution. In this work, the minimum number of realizations for each day-ahead schedule ranges from 1877 to 2188 trials.

Since the main goal of the paper is to address the wind uncertainty, the load was considered deterministic. Also, the load uncertainty is much lower than the wind uncertainty [68].

To assess the realistic performance of day-ahead schedules against the simulated realizations of uncertainty, a Monte Carlo simulation is performed for each realization of uncertainty. To meet each of these realizations, the re-dispatch and re-commitment decisions are modeled to reflect the intra-day actions of system operators. The re-dispatch decisions allow changes to the power output of committed generators, if constraints on the minimum and maximum generation output, up and down ramp rates, and power flow limits are met. The re-commitment decisions assume that adjustments to the day-ahead binary decisions can be performed on the day, if the inter-temporal constraints (2)–(6) are not violated. Since this paper focuses on the reliability UC process in the context of a vertically integrated utility, the real-time re-dispatch and re-commitment decisions are priced at the marginal start up and fuel cost of generators. However, if the re-dispatch and re-commitment decisions are insufficient, avoiding infeasibility may require load shedding, which is penalized in the objective function at \$10/kWh. We refer interested readers to [41] for further reading on the impacts of the value of the load shedding penalty on the day-ahead schedule.

Fig. 4 shows the cumulative probability distribution functions (CDF) of the expected operating cost as calculated using Monte Carlo simulations for the various test cases and the four UC formulations. In all the cases, regardless of the generator characteristics and the wind penetration, the SUC formulation is the most cost-effective. IIUC is second best, followed by RUC, while IUC is the least cost-effective. The IIUC has a more significant advantage over the RUC for the unfavorable wind profile, as can be seen in parts (B) and (D) of Fig. 4. The poor performance of the IUC is more notable for the favorable wind profiles in parts (A) and (C).

Table I compares the cost performance of the SUC, IIUC, RUC, and IUC models in terms of the expected cost (EC) and the standard deviation (SD) of the cost distribution obtained using the Monte Carlo simulations. The expected cost (EC) is the mean value of the CDF shown in Fig. 4, while the standard deviation (SD) presents the expected deviation from this value in percentages. For each case, the SD is also calculated in percentage of its corresponding EC.

The EC of each UC model decreases as wind penetration increases. Test system G2 consistently results in a lower value of the EC due to its less stringent minimum up and down time constraints on generators than in test system G1. This difference increases with the wind penetration level. Fig. 5 compares the cost of the IIUC, IUC, and RUC models with the cost of the SUC model. For the 10% wind penetration case, the IIUC solution costs less than 0.5% more than the SUC. On the other hand, the RUC and IUC cost up to 0.8% and 2.0% more. For a 20% wind penetration, the expected cost with the IIUC, RUC and IUC are up to 0.8%, 1.2% and 5.0% higher. These differences in cost grow further as the wind penetration increases.

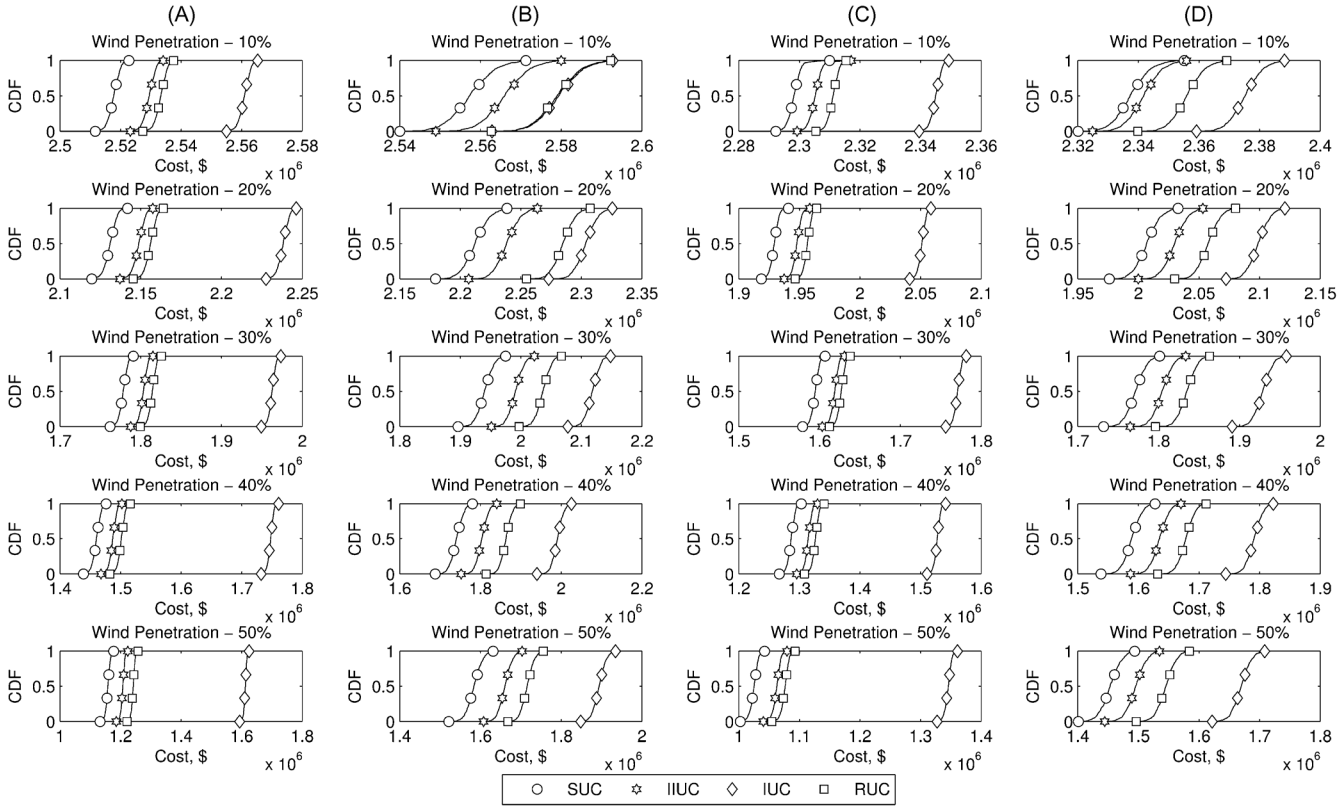

Fig. 4. Comparison of expected operating costs of the day-ahead schedules obtained with the SUC, IIUC, IUC, and RUC ($\Gamma = \mathrm{card}(\Omega^{\mathrm{W}})$) for different wind penetration levels–(A) generator dataset G1, favorable wind profile; (B) generator dataset G1, unfavorable wind profile; (C) generator dataset G2, favorable wind profile; (D) generator dataset G2, unfavorable wind profile.

TABLE I
COMPARISON OF THE COST PERFORMANCE (EC—EXPECTED COST; SD—STANDARD DEVIATION)

			10%		20%		30%		40%		50%	
			EC, $\cdot 10^6$\$	SD, $\cdot 10^3$\$ (%)	EC $\cdot 10^6$\$	SD, $\cdot 10^3$\$ (%)	EC, $\cdot 10^6$\$	SD, $\cdot 10^3$\$ (%)	EC, $\cdot 10^6$\$	SD, $\cdot 10^3$\$ (%)	EC, $\cdot 10^6$\$	SD, $\cdot 10^3$\$ (%)
G1	Favorable	SUC	2.518	1.928 (0.08%)	2.131	3.721 (0.17%)	1.778	5.070 (0.29%)	1.460	6.651 (0.46%)	1.158	7.345 (0.63%)
		IIUC	2.529	1.919 (0.08%)	2.149	3.609 (0.17%)	1.803	4.837 (0.27%)	1.487	5.902 (0.40%)	1.207	6.350 (0.53%)
		RUC*	2.533	1.846 (0.07%)	2.156	3.391 (0.16%)	1.814	4.631 (0.26%)	1.501	5.770 (0.38%)	1.241	6.002 (0.48%)
		IUC	2.561	1.846 (0.07%)	2.238	3.356 (0.15%)	1.963	4.224 (0.22%)	1.758	6.937 (0.40%)	1.612	4.838 (0.30%)
	Unfavorable	SUC	2.557	5.429 (0.21%)	2.212	10.340 (0.47%)	1.940	12.997 (0.67%)	1.741	15.540 (0.89%)	1.584	18.253 (1.15%)
		IIUC	2.566	5.324 (0.21%)	2.239	9.611 (0.43%)	1.991	12.166 (0.61%)	1.804	14.334 (0.79%)	1.661	15.958 (0.96%)
		RUC*	2.579	5.128 (0.20%)	2.285	8.663 (0.38%)	2.037	11.719 (0.58%)	1.863	13.564 (0.73%)	1.716	15.324 (0.89%)
		IUC	2.580	5.188 (0.20%)	2.304	8.594 (0.37%)	2.118	11.397 (0.54%)	1.991	13.540 (0.68%)	1.894	15.213 (0.80%)
G2	Favorable	SUC	2.298	5.678 (0.10%)	1.929	9.742 (0.18%)	1.595	11.951 (0.30%)	1.286	14.411 (0.47%)	1.025	16.232 (0.64%)
		IIUC	2.305	5.359 (0.10%)	1.948	9.285 (0.18%)	1.619	11.610 (0.29%)	1.315	13.680 (0.43%)	1.063	15.529 (0.59%)
		RUC*	2.311	5.073 (0.08%)	1.957	8.607 (0.16%)	1.627	10.932 (0.28%)	1.326	12.931 (0.42%)	1.076	14.854 (0.57%)
		IUC	2.345	5.071 (0.07%)	2.051	8.418 (0.15%)	1.771	10.756 (0.25%)	1.527	12.757 (0.33%)	1.345	14.587 (0.41%)
	Unfavorable	SUC	2.338	2.307 (0.24%)	2.007	3.555 (0.49%)	1.772	4.768 (0.67%)	1.589	5.989 (0.91%)	1.438	6.511 (1.12%)
		IIUC	2.342	2.299 (0.23%)	2.030	3.520 (0.46%)	1.805	4.721 (0.64%)	1.635	5.697 (0.84%)	1.496	6.268 (1.04%)
		RUC*	2.356	1.785 (0.22%)	2.058	3.154 (0.42%)	1.835	4.578 (0.60%)	1.678	5.539 (0.77%)	1.545	6.170 (0.96%)
		IUC	2.375	1.757 (0.21%)	2.099	3.107 (0.40%)	1.929	4.468 (0.56%)	1.791	5.052 (0.71%)	1.670	5.560 (0.87%)

$*$—RUC is solved with $\Gamma = \mathrm{card}(\Omega^{\mathrm{W}})$

Using IUC may result in up to 39% higher operating cost as compared to SUC. At 4.8% and 8.3%, respectively, the worst IIUC and RUC cost increases are much lower. This comparison of the cost-performance of various UC models supports the usefulness of the proposed IIUC model, which reduces the unnecessary conservatism of the RUC and IUC models by modeling realistic ramping scenarios.

As discussed in [41], the SD can be used to characterize the adaptability of the day-ahead schedule to the true realization of uncertainty. Thus, if the SD is high, the day-ahead schedule may require expensive corrective actions for some realizations of wind. On the other hand, the absolute and relative values of the SD tend to increase with wind penetration, which indicates that all UC models considered become more sensitive to deviations from the central forecast under high wind penetra-

TABLE II
COMPARISON OF ENERGY IMBALANCES (EWS—EXPECTED WIND SPILLAGE; EENS—EXPECTED ENERGY NOT SERVED)

			10%		20%		30%		40%		50%	
			EWS, MWh	EENS, MWh (freq.)	EWS, MWh	EENS, MWh (freq.)	EWS, MWh	EENS, MWh (freq.)	EWS, MWh	EENS, MWh (freq.)	EWS, MWh	EEN,S MWh (freq.)
G1	Favorable	SUC	0	0.009 (1)	0	0.008 (6)	0	0.005 (6)	20	0 (0)	62	0 (0)
		IIUC	0	0.001 (2)	0	0 (0)	0	0 (0)	0	0 (0)	59	0 (0)
		RUC*	0	0 (0)	0	0 (0)	0	0 (0)	8	0 (0)	383	0 (0)
		IUC	0	0 (0)	0	0 (0)	0	0 (0)	3	0 (0)	3,294	0 (0)
	Unfavorable	SUC	0	0.007 (6)	16	0.004 (2)	1,124	0 (0)	5,044	0 (0)	12,161	0 (0)
		IIUC	0	0 (0)	20	0 (0)	1,134	0 (0)	5,215	0 (0)	12,736	0 (0)
		RUC*	0	0 (0)	98	0 (0)	1,717	0 (0)	6,845	0 (0)	14,427	0 (0)
		IUC	0	0 (0)	16	0 (0)	2,457	0 (0)	10,166	0 (0)	19,735	0 (0)
G2	Favorable	SUC	0	0.045 (22)	0	0.038 (21)	0	0.012 (9)	9	0.009 (8)	211	0.008 (6)
		IIUC	0	0.043 (17)	0	0.034 (14)	0	0.011 (8)	1	0.007 (6)	151	0 (0)
		RUC*	0	0 (0)	0	0 (0)	0	0 (0)	2	0 (0)	271	0 (0)
		IUC	0	0 (0)	0	0 (0)	0	0 (0)	3	0 (0)	444	0 (0)
	Unfavorable	SUC	0	0.035 (17)	31	0.033 (20)	1,965	0.021 (10)	6,432	0.021 (18)	13,462	0.010 (10)
		IIUC	0	0 (0)	40	0 (0)	1,973	0 (0)	6,527	0 (0)	13,846	0 (0)
		RUC*	0	0 (0)	118	0 (0)	2,366	0 (0)	7,396	0 (0)	15,080	0 (0)
		IUC	0	0 (0)	67	0 (0)	2,883	0 (0)	9,650	0 (0)	18,099	0 (0)

∗—RUC is solved with $\Gamma = \mathrm{card}(\Omega^{\mathrm{W}})$

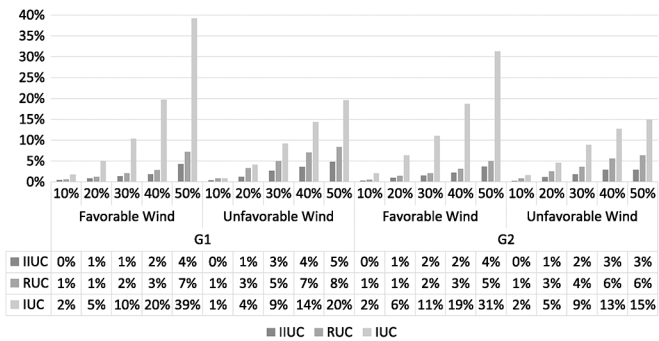

Fig. 5. Increase in the expected costs of the schedules produced by the IIUC, RUC ($\Gamma = \mathrm{card}(\Omega^{\mathrm{W}})$) and IUC as compared to the SUC for different wind penetration levels.

tion levels. The SD also depends on the temporal correlation between wind generation and load. If this correlation is favorable, all UC models under any wind penetration level have a lower SD than under the unfavorable correlation. As shown in Table I, the day-ahead schedule obtained using the SUC model results in the largest SD among all UC models for any wind profile, wind penetration level, and test system. On the other hand, the IUC approach systematically results in the lowest SD among all UC models considered. We conclude that the conservative formulations (IUC and RUC) are more adaptive to the extreme realizations of uncertainty than the IIUC and IUC models.

Table II shows the expected wind spillage (EWS) and expected energy not served (EENS) observed at each simulation. These outcomes are also quantified by the frequency of their occurrence. This frequency, denoted as freq. in Table II, is defined as the number of samples in Monte Carlo simulations where load is shed during at least one operating hour.

EWS is much lower for the favorable wind scenario as compared to the unfavorable one. For the favorable wind profile there is no wind spillage observed for all UC techniques for up to 30% wind energy penetration. Starting at the 40% wind energy penetration, some wind energy is spilled with almost all techniques. The proposed IIUC model results in the least EWS among all UC models for the favorable wind profile under 40% and 50% wind penetration levels. This outcome indicates the proposed IIUC model outperforms other UC models in terms the total usage of available wind generation and, thus, facilitates cost-effective scheduling and dispatch under high wind penetration levels. On the other hand, the day-ahead schedule obtained using the IUC model leads to unnecessarily high EWS of 3294 MWh for the G1 generator dataset at 50% wind penetration and for the favorable wind profile. This excessive wind spillage is mainly caused by the day-ahead IUC schedule being very much protected against load shedding. In this case, the IUC model commits a large number of generators to be able to serve all loads under a low production of wind farms, so that wind spillage is necessary to meet their minimum output constraints enforced by (11). Comparing the wind spillage occurred under the day-ahead IUC and IIUC models, it can be seen that the approach to model ramping scenarios as proposed in the IIUC paper is more realistic than overly conservative ramp requirements in the IUC model. For the unfavorable wind profile, the SUC model consistently results in the lowest EWS observed, while wind spillage under the day-ahead IIUC schedule almost always results in the second least wind spillage, especially for higher wind penetrations. The RUC and IUC models result in a substantially larger wind spillage as compared to the SUC and IIUC models. This observation illustrates the claim that conservatism of UC approaches modeling the range of uncertainty must be controlled by modeling realistic ramp requirements, as proposed in this paper.

Since the IUC and RUC with $\Gamma = \mathrm{card}(\Omega^{W})$ models are conservative, they result in no load shedding (EENS= 0 MWh) regardless of the chosen test case parameters, wind penetration, and wind profile (Table II). On the other hand, the SUC solution is drawn from the set of 10 scenarios, which may not protect it against some extreme outcomes, and thus may lead to some load shedding under almost all wind penetration levels. As can be observed in Table II, the EENS of the SUC model decreases

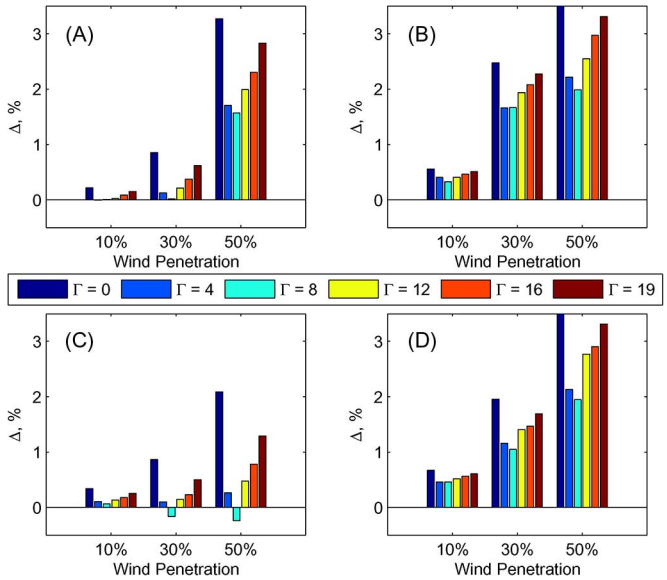

Fig. 6. Difference in the expected costs of the schedules produced by the IIUC and RUC with different budgets of uncertainty Γ—(A) generator dataset G1, favorable wind profile; (B) generator dataset G1, unfavorable wind profile; (C) generator dataset G2, favorable wind profile; (D) generator dataset G2, unfavorable wind profile.

as the wind penetration increases. For higher wind penetrations, more fast-starting generators remain uncommitted on the day ahead and thus can be synchronized in real time to avoid shedding load. Furthermore, load shedding under the SUC solution for the favorable wind profile and wind penetration up to 20% case tends to be larger than for the unfavorable wind profile. We also observe that there is no systematic relation between the magnitude of the EENS and the frequency of load shedding, i.e., EENS can be higher for a lower frequency and vice-versa. Additionally, it avoids load shedding for high wind penetrations and the favorable wind profile. However, in these cases load shedding is also dependent on the flexibility of the generation mix. Test system G1 incurs less load shedding than test system G2. Although in some simulations the IIUC model results in load shedding, the EENS in these cases is lower than for the SUC schedule. The load shedding statistics for the IIUC and SUC shows that modeling of ramping scenarios in the IIUC model tends to reduce the EENS and its frequency as compared to the SUC. Comparing the results in Tables I and II, it can be seen that UC models with higher EC and lower SD tend to result in lower EENS. This observation is consistent with [41], which explains the sensitivity of UC models to the load shedding penalty.

D. Comparison of the IIUC Model and the RUC Model With Different Values of Γ

While the budget of uncertainty Γ can be used to regulate the conservatism of the RUC model, there is no systematic approach to choose the most cost-effective Γ before solving the optimization problem. Fig. 6 compares the difference between the expected cost of the IIUC and RUC with different values of Γ. This difference is calculated as $\Delta = (EC_{\Gamma}^{\mathrm{RUC}} - EC^{\mathrm{IIUC}})/EC^{\mathrm{IIUC}} \cdot 100\%$, where $EC_{\Gamma}^{\mathrm{RUC}}$ is the expected cost of the RUC model for a given budget of uncertainty Γ and EC^{IIUC} is the expected cost of the IIUC model. $EC_{\Gamma}^{\mathrm{RUC}}$ decreases as Γ increases and reaches its minimum for $\Gamma = 8$. Increasing Γ beyond 8 results in more conservative schedules and $EC_{\Gamma}^{\mathrm{RUC}}$ increases. As compared to the IIUC, the RUC model consistently results in a more expensive solution, except for cases with 30% and 50% wind penetration in test system G2 with favorable wind profile. It can also be seen in Fig. 6 that Δ, i.e., the cost savings achieved with the proposed IIUC model, increases with wind penetration for each case considered.

Table III summarizes the cost and reliability performance of the least-cost RUC schedule ($\Gamma = 8$). The least-cost RUC model tends to trade-off the EC, SD, EWS, and EENS performance of the IIUC model and the RUC model with $\Gamma = 19$. In most of the cases the least-cost RUC model remains more expensive and conservative than the IIUC model. On the other hand, there are two cases, also shown in Fig. 3, where the least-cost RUC model outperforms the IIUC model in terms of the EC (these cases are shown in bold in Table III). However, a lower EC as compared to the IIUC also leads to a larger SD, which indicates that reducing the value of the budget of uncertainty also decreases the ability of the RUC model to deal with uncertainty. Furthermore, in case of the generator dataset G2, favorable wind profile and 30% wind penetration, the least-cost RUC solution results in larger and more frequent load shedding than the IIUC model. These observations suggest that the value of the budget of uncertainty should be carefully tuned to ensure that a potential reduction in the EC does not worsen the reliability performance of the RUC model.

E. Computation Efficiency

All the simulations were carried out using CPLEX 12.1 run under the GAMS 23.7 environment on an Intel i7 1.8-GHz processor with 4 GB of memory. To improve numerical stability and avoid convergence issues [43]–[46], as well as their effect on the cost performance of different UC formulations, this paper does not implement advanced solution techniques, such as those discussed in [42]. Therefore, the results of this case study should

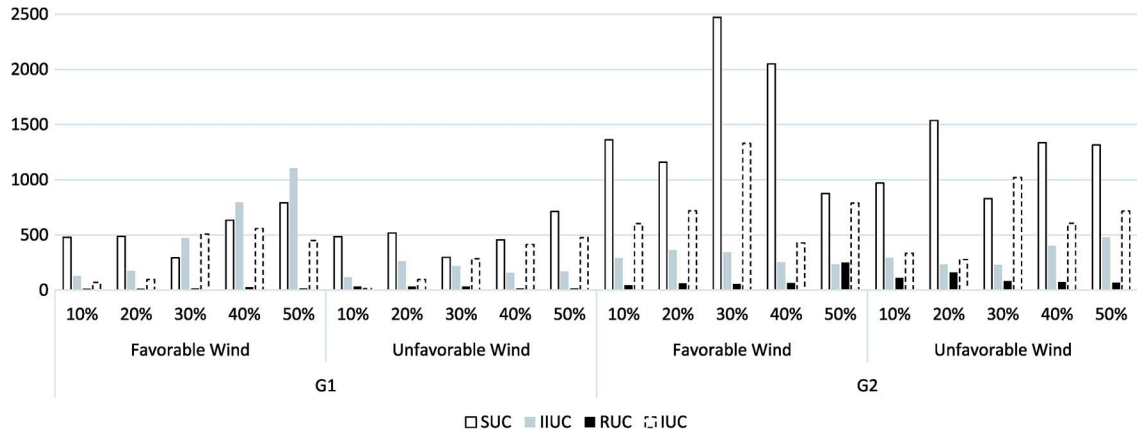

Fig. 7. Wall-clock times in seconds required to reach 1% optimality gap for different wind penetration levels.

TABLE III
COST AND RELIABILITY PERFORMANCE OF THE RUC MODEL FOR $\Gamma = 8$. (EC—EXPECTED COST; SD—STANDARD DEVIATION OF THE COST; EWS—EXPECTED WIND SPILLAGE; EENS—EXPECTED ENERGY NOT SERVED)

			10%	30%	50%
G1	Favorable	EC, $\cdot 10^6$\$	2.530	1.805	1.226
		SD, $\cdot 10^3$\$	1.851	4.706	6.097
		(%)	(0.07%)	(0.26%)	(0.49%)
		EWS, MWh	0	0	2,114
		EENS, MWh (freq.)	0.001 (2)	0 (0)	0 (0)
	Unfavorable	EC, $\cdot 10^6$\$	2.574	2.025	1.694
		SD, $\cdot 10^3$\$	5.201	11.803	15.612
		(%)	(0.20%)	(0.58%)	(0.92%)
		EWS, MWh	0	1,810	16,107
		EENS, MWh (freq.)	0 (0)	0 (0)	0 (0)
G2	Favorable	EC, $\cdot 10^6$\$	2.307	**1.616**	**1.060**
		SD, $\cdot 10^3$\$	5.340	**11.710**	**15.618**
		(%)	(0.23%)	**(0.72%)**	**(1.47%)**
		EWS, MWh	0	**0**	**191**
		EENS, MWh (freq.)	0.040 (14)	**0.013 (9)**	**0 (0)**
	Unfavorable	EC, $\cdot 10^6$\$	2.353	1.824	1.525
		SD, $\cdot 10^3$\$	1.911	4.403	6.300
		(%)	(0.08%)	(0.24%)	(0.41%)
		SD, $\cdot 10^3$\$ (%)	1.911	4.403	6.300
		EWS, MWh	0	2,104	14,882
		EENS, MWh (freq.)	0 (0)	0 (0)	0 (0)

Bold denotes the cases when the RUC model with $\Gamma = 8$ outperforms the IIUC model in terms of the expected cost.

be interpreted as providing an upper bound on the computing performance. Fig. 7 shows the wall-clock times in seconds required to reach a 1% optimality gap. Overall, RUC is by far the most efficient method. For the G1 generator dataset, the IIUC and IUC perform similarly, while for the G2 dataset, the IIUC outperforms IUC in 80% of the cases. SUC is the most computationally demanding method, except for 30%–50% wind penetration levels applied to G1 dataset and favorable wind.

IV. CONCLUSIONS

The numerical results presented in this paper show that the SUC is still the most cost-effective way of dealing with wind uncertainty. However, despite the small number of scenarios (10) considered, its computational burden is generally very high. The proposed IIUC is the second best option in terms of cost-effectiveness (the average operating cost is increased by 2.0%) and a much better option in terms of computing time (the average computing time is reduced by 53%). The operating cost of RUC schedules is on average 3.5% higher than the one of SUC schedules, but the computing times are reduced by 93% in average. The IUC is the least attractive method because the average expected operating cost is 11.8% higher than the SUC, and computing time is reduced only by 41% as compared to the SUC.

ACKNOWLEDGMENT

The authors would like to thank Dr. D. I. Sun and Dr. X. Wang of Alstom Grid, Prof. M. A. Ortega-Vazquez of the University of Washington, and anonymous reviewers for discussions, thoughtful suggestions, and constructive criticism of this paper.

REFERENCES

[1] Y. V. Makarov, C. Loutan, M. Jian, and P. de Mello, "Operational impacts of wind generation on California power systems," *IEEE Trans. Power Syst.*, vol. 24, no. 2, pp. 1039–1050, May 2009.
[2] E. Ela and M. O'Malley, "Studying the variability and uncertainty impacts of variable generation at multiple timescales," *IEEE Trans. Power Syst.*, vol. 27, no. 3, pp. 1324–1333, Aug. 2012.
[3] N. Growe-Kuska, H. Heitsch, and W. Romisch, "Scenario reduction and scenario tree construction for power management problems," in *Proc. 2003 IEEE Power Tech Conf.*, Bologna, Italy, Jun. 2003, pp. 1–7.
[4] M. Lange, "On the uncertainty of wind power predictions-analysis of the forecast accuracy and statistical distribution of errors," *J. Sol. Energy Eng.*, vol. 127, no. 2, pp. 177–184, 2005.
[5] Y. Dvorkin, M. A. Ortega-Vazquez, and D. S. Kirschen, "Assessing flexibility requirements in power systems," *IET Gener., Transm., Distrib.*, vol. 8, no. 11, pp. 1820–1830, Nov. 2014.
[6] M. A. Ortega-Vazquez and D. S. Kirschen, "Assessing the impact of wind power generation on operating costs," *IEEE Trans. Smart Grid*, vol. 1, no. 3, pp. 295–301, Dec. 2010.
[7] J. Ma, V. Silva, R. Belhomme, D. S. Kirschen, and L. F. Ochoa, "Evaluating and planning flexibility in sustainable power systems," *IEEE Trans. Sustain. Energy*, vol. 4, no. 1, pp. 200–209, Jan. 2013.
[8] A. J. Wood and B. F. Wollenberg, *Power Generation, Operation, Control*. New York, NY, USA: Wiley, 1984.

[9] Y. G. Rebours, D. S. Kirschen, M. Trotignon, and S. Rossignol, "A survey of frequency and voltage control ancillary services. part I: Technical features," *IEEE Trans. Power Syst.*, vol. 22, no. 1, pp. 350–357, Feb. 2007.

[10] Y. G. Rebours, D. S. Kirschen, M. Trotignon, and S. Rossignol, "A survey of frequency and voltage control ancillary services. part II: Economic features," *IEEE Trans. Power Syst.*, vol. 22, no. 1, pp. 358–366, Feb. 2007.

[11] ERCOT Methodologies for Determining Ancillary Service Requirements, 2012 [Online]. Available: www.ercot.com/meetings/wms/keydocs/2004/0819/WMS08192004-3.doc

[12] R. Piwko, K. Clark, L. Freeman, G. Jordan, and N. Miller, Western Wind and Solar Integration Study, 2010.

[13] M. A. Ortega-Vazquez and D. S. Kirschen, "Optimizing the spinning reserve requirements using a cost/benefit analysis," *IEEE Trans. Power Syst.*, vol. 22, no. 1, pp. 24–33, Feb. 2007.

[14] M. A. Ortega-Vazquez, D. S. Kirschen, and D. Pudjianto, "Optimising the scheduling of spinning reserve considering the cost of interruptions," *IEE Proc. Gener., Transm., Distrib.*, vol. 153, no. 5, pp. 570–575, Sept. 2006.

[15] F. D. Galiana, F. Bouffard, J. M. Arroyo, and J. F. Restrepo, "Scheduling and pricing of coupled energy and primary, secondary, tertiary reserves," *Proc. IEEE*, vol. 93, no. 11, pp. 1970–1983, Nov. 2005.

[16] J. M. Arroyo and F. D. Galiana, "Energy and reserve pricing in security and network-constrained electricity markets," *IEEE Trans. Power Syst.*, vol. 20, no. 2, pp. 634–643, May 2005.

[17] M. A. Ortega-Vazquez and D. S. Kirschen, "Should the spinning reserve procurement in systems with wind power generation be deterministic or probabilistic?," in *Proc. Sustainable Power Generation and Supply '09*, Nanjing, China, Apr. 2009, pp. 1–9.

[18] F. Bouffard, F. D. Galiana, and A. J. Conejo, "Market-clearing with stochastic security-part I: Formulation," *IEEE Trans. Power Syst.*, vol. 20, no. 4, pp. 1818–1826, Nov. 2005.

[19] F. Bouffard, F. D. Galiana, and A. J. Conejo, "Market-clearing with stochastic security-part II: Case studies," *IEEE Trans. Power Syst.*, vol. 20, no. 4, pp. 1827–1835, Nov. 2005.

[20] J. M. Morales, R. Minguez, and A. J. Conejo, "A methodology to generate statistically dependent wind speed scenarios," *Appl. Energy*, vol. 87, no. 3, pp. 843–855, Mar. 2010.

[21] S. Takriti, J. R. Birge, and E. Long, "A stochastic model for the unit commitment problem," *IEEE Trans. Power Syst.*, vol. 11, no. 3, pp. 1497–1508, Aug. 1996.

[22] P. Carpentier, G. Gohen, J. C. Culioli, and A. Renaud, "Stochastic optimization of unit commitment: A new decomposition framework," *IEEE Trans. Power Syst.*, vol. 11, no. 2, pp. 1067–1073, May 1996.

[23] J. Wang, M. Shahidehpour, and Z. Li, "Security-constrained unit commitment with volatile wind power generation," *IEEE Trans. Power Syst.*, vol. 23, no. 3, pp. 1319–1327, Aug. 2008.

[24] L. Wu and M. Shahidehpour, "Accelerating the Benders decomposition for network-constrained unit commitment problems," *Energy Syst.*, vol. 1, no. 3, pp. 339–376, 2010.

[25] L. Wu, M. Shahidehpour, and T. Li, "Stochastic security-constrained unit commitment," *IEEE Trans. Power Syst.*, vol. 22, no. 2, pp. 800–811, May 2007.

[26] A. J. Conejo, M. Carrion, and J. M. Morales, *Decision Making Under Uncertainty in Electricity Markets*. New York, NY, USA: Springer, 2010.

[27] A. Papavasiliou, S. S. Oren, and B. Rountree, Applying High Performance Computing to Transmission-Constrained Stochastic Unit Commitment for Renewable Energy Integration, 2012 [Online]. Available: http://www.ieor.berkeley.edu/ oren/pubs/Tony-PES-HPC-Final.pdf

[28] J. Dupačová, N. Gröwe-Kuska, and W. Römisch, "Scenario reduction in stochastic programming," *Math. Program.*, vol. 95, pp. 493–511, Feb. 2003.

[29] H. Heitsch and W. Römisch, "Scenario reduction algorithms in stochastic programming," *Comput. Optim. Appl.*, vol. 24, no. 2–3, pp. 187–206, Feb. 2003.

[30] J. M. Morales, S. Pineda, A. J. Conejo, and M. Carrion, "Scenario reduction for futures market trading in electricity markets," *IEEE Trans. Power Syst.*, vol. 24, no. 2, pp. 878–888, May 2009.

[31] L. Wu, M. Shahidehpour, and Z. Li, "Comparison of scenario-based and interval optimization approaches to stochastic SCUC," *IEEE Trans. Power Syst.*, vol. 27, no. 2, pp. 913–921, May 2012.

[32] Y. Dvorkin, Y. Wang, H. Pandžić, and D. S. Kirschen, "Comparison of scenario reduction techniques for the stochastic unit commitment," in *Proc. IEEE PES General Meeting 2014*, Jul. 2014, pp. 1–5.

[33] S. M. Ryan, R. J. B. Wets, D. L. Woodruff, C. Silva-Monroy, and J. P. Watson, "Toward scalable, parallel progressive hedging for stochastic unit commitment," in *Proc. IEEE PES General Meeting 2013*, Vancouver, BC, Canada, Jul. 2013, pp. 1–5.

[34] D. Bertsimas, E. Litvinov, X. A. Sun, Z. Jinye, and Z. Tongxin, "Adaptive robust optimization for the security constrained unit commitment problem," *IEEE Trans. Power Syst.*, vol. 28, no. 1, pp. 52–63, Feb. 2013.

[35] R. Jiang, M. Zhang, G. Li, and Y. Guan, "Two-stage network constrained robust unit commitment problem," *Eur. J. Oper. Res.*, vol. 234, no. 3, pp. 751–762, May 2014.

[36] R. Jiang, J. Wang, M. Zhang, and Y. Guan, "Two-stage minimax regret robust unit commitment," *IEEE Trans. Power Syst.*, vol. 28, no. 3, pp. 2271–2282, Aug. 2013.

[37] R. Jiang, J. Wang, and Y. Guan, "Robust unit commitment with wind power and pumped storage hydro," *IEEE Trans. Power Syst.*, vol. 27, no. 2, pp. 800–810, May 2012.

[38] B. Zheng and L. Zhao, "Robust unit commitment problem with demand response and wind energy," in *Proc. IEEE PES General Meeting 2012*, San Diego, CA, USA, Jul. 2012, pp. 1–8.

[39] B. Zeng and L. Zhao, "Solving two-stage robust optimization problems using a column-and-constraint generation method," *Oper. Res. Lett.*, vol. 41, no. 5, pp. 457–461, 2013.

[40] C. Zhao and Y. Guan, "Unified stochastic and robust unit commitment," *IEEE Trans. Power Syst.*, vol. 28, no. 3, pp. 3353–3361, Aug. 2013.

[41] Y. Dvorkin, H. Pandžić, M. Ortega-Vazquez, and D. S. Kirschen, "A hybrid stochastic/interval approach to transmission-constrained unit commitment," *IEEE Trans. Power Syst.*, to be published.

[42] Q. Zheng, J. Wang, and M. A. Liu, "Stochastic optimization for unit commitment—a review," *IEEE Trans. Power Syst.*, to be published.

[43] A. Papavasiliou and S. S. Oren, "A comparative study of stochastic unit commitment and security-constrained unit commitment using high performance computing," in *Proc. 2013 European Control Conf. (ECC)*, 2013, pp. 2507–2512.

[44] V. Zavala, M. Anitescu, A. Kannan, and C. Petr, On the Convergence of day—Ahead and Real—Time Electricity Markets, FERC [Online]. Available: http://www.ferc.gov/CalendarFiles/20110628130756-Jun28-SesC3-Zavala-Argonne.pdf, 2011

[45] G. Anders, Commitment Techniques for Combined-Cycle Generating Units, NYISO, 2005 [Online]. Available: http://tinyurl.com/kw5w5l7

[46] P. Bendotti, C. DAmbrosio, G. Doukopoulos, A. Lenoir, L. Liberti, and Y. Sahraoui, "MILP model for a real-world hydro-power unit-commitment problem," in *Proc. 2014 Mixed Integer Programming Workshop*, 2014 [Online]. Available: http://tinyurl.com/lyu5bca

[47] X. Sun and C. Fang, "Interval mixed-integer programming for daily unit commitment and dispatch incorporating wind power," in *Proc. Power System Technology (POWERCON) 2010*, Hangzhou, China, Oct. 2010, pp. 1–6.

[48] Y. Wang, Q. Xia, and C. Kang, "Unit commitment with volatile node injections by using interval optimization," *IEEE Trans. Power Syst.*, vol. 26, no. 3, pp. 1705–1713, Aug. 2011.

[49] D. Rajan and S. Takriti, Minimum up/Down Polytopes of the Unit Commitment Problem With Start-up Costs, IBM Res. Rep., Jun. 2005.

[50] Transpower, Resolving Infeasibilities & High Spring Washer Price situations—An Overview, Tech. Rep., 2010 [Online]. Available: http://tinyurl.com/ndqoy8f

[51] A. Lorca and X. A. Sun, "Adaptive robust optimization with dynamic uncertainty sets for multi-period economic dispatch under significant wind," *IEEE Trans. Power Syst.*, to be published.

[52] Reliability Task Force of the Application of Probability Methods Subcommittee, "The IEEE Reliability Test System—1996," *IEEE Trans. Power Syst.*, vol. 14, no. 3, pp. 1010–1020, Aug. 1999.

[53] REAL Library, University of Washington [Online]. Available: www.ee.washington.edu/research/real/library.html

[54] H. Pandžić, T. Qiu, and D. Kirschen, "Comparison of state-of-the-art transmission constrained unit commitment formulations," in *Proc. IEEE PES General Meeting 2013*, Vancouver, BC, Canada, Jul. 2013, pp. 1–5.

[55] M. Ortega-Vazquez, "Optimizing the spinning reserve requirements," Ph.D. dissertation, Univ. Manchester, Manchester, U.K., May 2006.

[56] P. Pinson and H. Madsen, "Ensemble-based probabilistic forecasting at Horns Rev," *Wind Energy*, vol. 12, no. 2, pp. 137–155, 2009.

[57] R. Jursa, "Wind power prediction with different artificial intelligence models," in *Proc. 2007 Eur. Wind Energy Conf.*, Milan, Italy, May 2007.

[58] T. Hastie, R. Tibshirani, and J. Friedman, *The Elements of Statistical Learning: Data Mining, Inference and Prediction*, 2nd ed. New York, NY, USA: Springer, 2009.
[59] A. J. Smola and B. Schlkopf, "A tutorial on support vector regression," *Statist. Comput.*, vol. 14, no. 3, pp. 199–222, Aug. 2004.
[60] G. Giebel, The State of the Art in Short-Term Prediction of Wind Power—A Literature Review, 2011,2nd ed. [Online]. Available: http://www.prediktor.dk/publ/GGiebelEtAl-StateOfTheArtInShort-TermPrediction_ANEMOSplus_2011.pdf
[61] L. Breiman, "Random forests," *Mach. Learn.*, vol. 45, no. 1, pp. 5–32, Oct. 2001.
[62] P. Pinson and G. Kariniotakis, "Conditional prediction intervals of wind power generation," *IEEE Trans. Power Syst.*, vol. 25, no. 4, pp. 1845–1856, Nov. 2010.
[63] C. W. Potter, D. Lew, J. McCaa, S. Cheng, S. Eichelberger, and E. Grimit, "Creating the dataset for the western wind and solar integration study," in *Proc. 7th Int. Workshop Large Scale Integration of Wind Power and on Transmission Networks for Offshore Wind Farms*, Madrid, Spain, May 2008, pp. 1–7.
[64] Q. Wang, Y. Guan, and J. Wang, "A chance-constrained two-stage stochastic program for unit commitment with uncertain wind power output," *IEEE Trans. Power Syst.*, vol. 27, no. 1, pp. 206–215, Feb. 2012.
[65] B. M. Hodge and M. Milligan, "Wind power forecasting error distributions over multiple timescales," in *Proc. IEEE PES General Meeting 2011*, Detroit, MI, USA, Jul. 24–29, 2011.
[66] M. S. Nazir and F. Bouffard, "Intra-hour wind power characteristics for flexible operations," in *Proc. IEEE PES General Meeting 2012*, San Diego, CA, USA, Jul. 2012, pp. 1–8.
[67] G. J. Hahn and S. S. Shapiro, *Statistical Models in Engineering*. New York, NY, USA: Wiley, 1967.
[68] A. Greenhall, "Wind scenarios for stochastic energy scheduling" Ph.D. dissertation, Univ. Washington, Seattle, WA, USA, 2013 [Online]. Available: http://www.hydrofoundation.org/pdf/greenhall-dissertation.pdf

Hrvoje Pandžić (S'06–M'12) received the M.E.E. and Ph.D. degrees from the Faculty of Electrical Engineering and Computing, University of Zagreb, Croatia, in 2007 and 2011, respectively.

During 2012–2014, he was a postdoctoral researcher at the University of Washington, Seattle, WA, USA. He is currently an Assistant Professor at the Faculty of Electrical Engineering and Computing, University of Zagreb, Croatia. His research interests include power system economics, integration of renewables, electric vehicles, and utilization of energy storage.

Yury Dvorkin (S'11) received the B.S.E.E degree with the highest honors at Moscow Power Engineering Institute (Technical University), Moscow, Russia, in 2011. He is pursuing the Ph.D. degree at the University of Washington, Seattle, WA, USA.

He is a recipient of the Clear Energy Institute's Graduate Fellowship. His research interests include operational and long-term flexibility in power systems, decision-making under uncertainty in power systems, power system analysis and operation, and power system economics.

Ting Qiu (S'12) received the B.S. degree in control science and engineering from Xian University of Technology, China, in 2008 and the M.Sc. degree in system engineering from Xian Jiaotong University, China, in 2011. She is currently pursuing the Ph.D. degree in electrical engineering at the University of Washington, Seattle, WA, USA.

Her research interests include optimization algorithms and their applications in electric power system and market operation.

Yishen Wang (S'12) received the B.S. degree from the Department of Electrical Engineering, Tsinghua University, Beijing, China, in 2011. He is currently pursuing the Ph.D. degree in electrical engineering at the University of Washington, Seattle, WA, USA.

His research interests include wind integration, wind forecasting, optimization techniques applied to power systems, and power system economics.

Daniel S. Kirschen (M'86–SM'91–F'07) received the electrical and mechanical engineer's degrees from the Université Libre de Bruxelles, Belgium, in 1979, and the M.Sc. and Ph.D. degrees from the University of Wisconsin, Madison, WI, USA, in 1980 and 1985, respectively.

He is currently Close Professor of Electrical Engineering at the University of Washington, Seattle, WA, USA. His research focuses on smart grids, the integration of renewable energy sources in the grid, power system economics, and power system security.